Research Article

Larah R. Abdulwahed*

Parametric study of retrofitted reinforced concrete columns with steel cages and predicting load distribution and compressive stress in columns using machine learning algorithms

https://doi.org/10.1515/cls-2022-0197
received January 04, 2023; accepted April 26, 2023

Abstract: Recently, the use of reinforced concrete (RC) structures is becoming very common worldwide. Because of earthquakes or poor design, some of these structures need to be retrofitted. Among different methods of retrofitting a structure, we have utilized a steel cage to support a column under axial load. The numerical modeling of a retrofitted column with a steel cage is carried out by the finite-element method in ABAQUS, and the effectiveness of the number of strips, size of strips, size of angles, RC head, the strips' thickness, and the steel cage's mechanical properties are studied on 15 different case studies by the single factorial method. These parameters proved to be very effective on the load distribution of the column because by choosing the optimum case, lower amounts of force are born by the column. By increasing the number of strips, the steel cage would reach 52% of the total load. This value for the size of strips and angles' size is 48 and 50%, respectively. However, the thickness of the strips does not have a significant effect on the load bearing of the column. In order to fully predict the load distribution of the retrofitted columns, the data of the present study are utilized to propose a predictive model for N_c/P_{FEM} and N_c/P_{FEM} using artificial neural networks. The model had an error of 1.56 (MAE), and the coefficient of determination was 0.97. This model proved to be so accurate that it could replace time-consuming numerical modeling and tedious experiments.

Keywords: reinforced concrete, steel cage, machine learning, numerical modeling, artificial neural network

*** Corresponding author: Larah R. Abdulwahed,** Technical Institute of Baquba, Middle Technical University, Diyala, Iraq,
e-mail: dr.larah.riyadh@mtu.edu.iq

1 Introduction

Nowadays, the attitude of engineers has changed from demolishing and renovating structures to retrofitting and upgrading due to the high cost [1,2]. Columns are one of the main elements of structures under axial shear force and bending moment, whose strength and ductility affect their seismic capacity. Currently, there are various methods for retrofitting reinforced concrete (RC) columns, including concrete coating [3–5], using fiber-reinforced polymer composites [6–8], and steel jackets [9–12]. The steel cage is considered a type of steel coating and is a simple, economical, and effective technique for strengthening rectangular and square cross-sections [13]. This method includes using four steel angles placed along the four corners of the column and forming the cage structure utilizing transverse strips welded to the fangs. The steel cage and the column gap are filled with cement or epoxy mortar. In the following, we will review some of the most important previous research in this field.

Frangou *et al.* [14] conducted a series of tests to strengthen RC columns through strapping, and the results showed an increase in the strength and ductility of the reinforced column. Aboutaha *et al.* [15] proved the efficiency of steel jackets connected to the column by the retaining screws in the RC column field by conducting experiments. Cirtek [16] reinforced a series of laboratory samples of RC columns using pre-tensioned steel strips, and the results showed an increase in the bearing capacity of the reinforced column. By conducting experiments on RC columns, Xiao and Wu [17] suggested using steel coating with hardeners at points prone to plastic joint formation to enhance the shear strength and ductility of the column. Wu *et al.* [18] evaluated more than 120 articles and results of more than 700 laboratory cases about different strengthening methods. They combined them with theoretical studies that proved that a steel cage is an effective method to augment the strength and ductility of RC columns. Adam *et al.* [19] proved the efficiency of the direct load transfer mechanism using steel pipes at the joint of the beam–column. Montuori and Piluso [20] presented a theoretical model that can predict the RC column. It was with an angle and a steel plate, which was highly accurate compared to the laboratory results. Adam *et al.* [21], using FEM and experimental studies, investigated the effective parameters on the behavior of RC columns reinforced with steel cages. Calderón *et al.* [22] proposed a novel approach based on the failure mechanism analysis obtained from the results and numerical and laboratory studies to measure the final load of the RC column retrofitted by steel cages. Tarabia and Albakry [23] proved the increase in the acceptable load and ductility of the reinforced column by conducting a series of tests on a RC column retrofitted with a steel cage. Belal *et al.* [24] investigated the behavior of RC columns retrofitted with steel cladding with laboratory and finite element studies and showed the effect of the number and size of strips used in the cladding on RC columns.

Although conventional methods are used to measure the response of structures against various forces [8,25–28], very few studies have been devoted to studying machine learning algorithms to predict the response of the structures [29–32]. In the current research, a retrofitted column using a steel cage is studied numerically. ABAQUS is used to model the column using the finite element method (FEM), and 15 cases are utilized. The single factorial method is used to look for the best case of study. Later, the data from this study are employed to propose artificial neural network (ANN) models for N_c/P_{FEM} and N_S/P_{FEM}. The results of the predictive models are studied by measuring parameters such as mean absolute error (MAE) and coefficient of determination. In order to fully optimize the neural networks, hyperparameter tuning is utilized. In this method, all the contributing parameters are refined in such a way that the best results are achieved.

2 Methods

The modeling of the present study has been done with ABAQUS. In order to model concrete parts, three-dimensional eight-node elements (C3D8R) from the continuum elements are utilized. Moreover, truss elements (T3D2) are employed for modeling rebars, and two-dimensional four-node elements (S4R) from the shell elements have been used to model cage components, including angles and sheets. The behavior of steel was defined as the behavior of an elastic–plastic material. An embedded region is used for the interaction between rebars and concrete, and tie constraints are used for welded connections. To define the non-linear behavior of concrete, the behavioral model of damaged concrete is used, and to define the uniaxial behavior curve of concrete, the behavioral model of Mander *et al.* [33] is used.

3 Specifications of laboratory models for calibration

Experimental studies have been selected to confirm the correctness of the numerical method and a better approach to the details of the FEM. In this article, we have selected a column reinforced with steel cages for parametric analysis, which will be described below.

3.1 Model under axial force

The experimental study chosen for this group is taken from the samples made by Adam [34] in the ICITECH Laboratory in Spain. The cross-section of the column is $300 \times 300\ \text{mm}^2$, and its height is 3,100 mm, reinforced with 12- and 6-grade rebars longitudinally and transversely. The column is reinforced with a steel angle bar and steel strip, and the cage is filled with sand and cement mortar between the column and the cage. Figure 1 shows the schematic model of the selected column. As can be seen, angles and strips are situated to support the column. Also, RC is used to support the structure better. Additionally, the RC head is used to strengthen the column, and the effect of that on the load bearing is investigated.

The RC column bears an axial force with a constant rate of 0.5 mm/min utilizing a hydraulic jack of 5,000 kN, and the force continues until the failure of the column. Tables 1–3 present the mechanical properties of the structures under the axial load.

4 Validation of the model

To evaluate the numerical modeling, the modeling results have been compared with the laboratory results. Figure 2 shows the FEM of the geometry.

In order to verify the results of the numerical modeling with the experimental results, the axial shortening of the column under the axial load is compared in Figure 3.

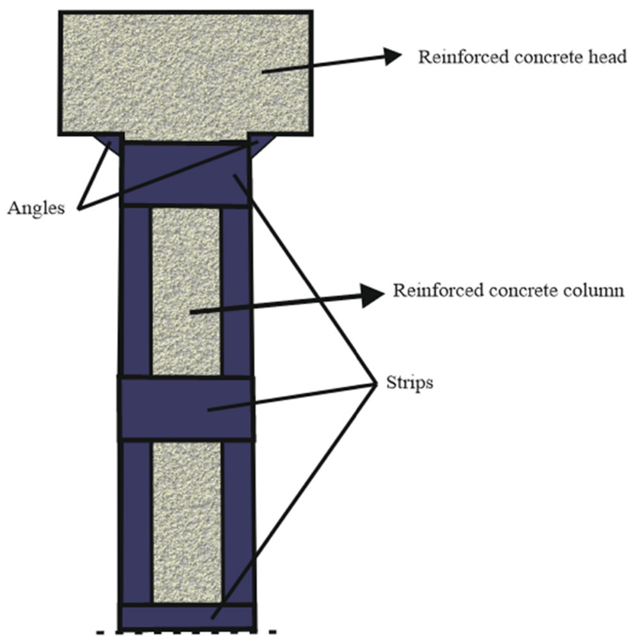

Figure 1: The schematic model of the RC column.

Table 1: Properties of concrete subjected to axial load

Structure	f'_c (MPa)	E_c (MPa)	ρ (kg/m^3)	v
Concrete	8.3	14,404	2,337	0.2

Table 2: Mechanical properties of the bar subjected to axial load

Structure	F_y (MPa)	E_s (GPa)	ρ (kg/m^3)	v
Longitudinal bar	400	210	7,850	0.3
Transverse bar	230	210	7,850	0.3

Adam's [34] experimental results have good coordination with the FEM results, which shows the appropriate accuracy of the software modeling.

5 Results

In the present study, we have modeled a column under an axial load and compared the impacts of various

Table 3: Properties of steel cage subjected to axial load

Structure	Angle	Strip	F_y (GPa)	E_s (GPa)	v
Steel cage	∟60.6	270 × 160 × 8	275	210	0.3

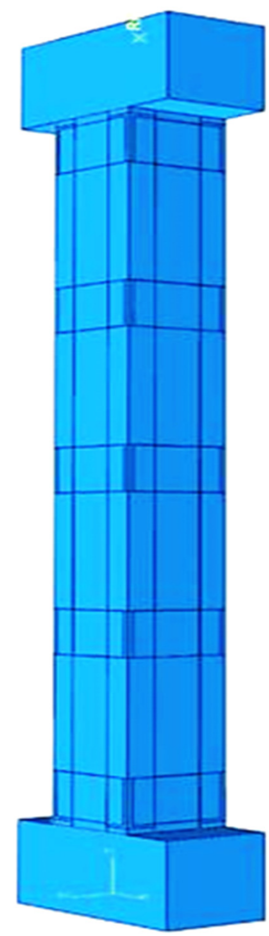

Figure 2: The geometry of the column.

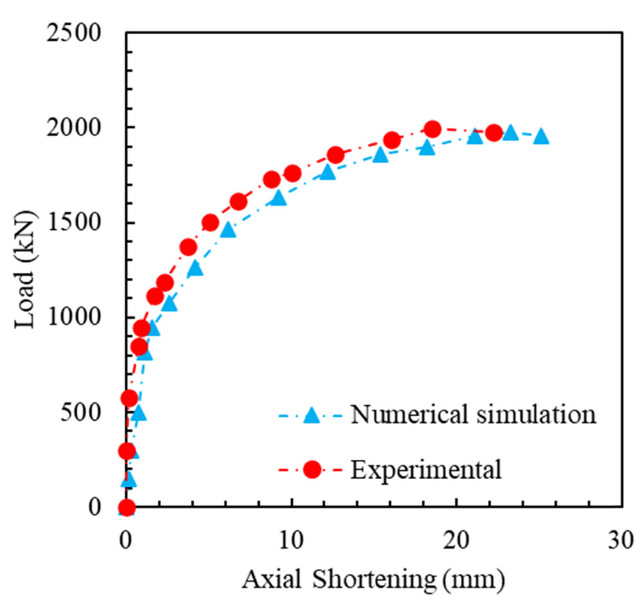

Figure 3: The validation of the numerical modeling using FEM and the experimental study of Adam [34].

parameters on the strength of the structure. Notably, the column is RC, and a steel cage is utilized for retrofitting the structure. The effects of the number and size of strips, size of bars, the thickness of strips, compressive strength of concrete, yield stress of cage, and the use of a head column at the column joint are investigated.

The load transfer mechanism is investigated between the RC column and the steel cage in the modeled samples. The indirect mode is where the load transfer occurs between the column and the cage through shear stresses and the mortar between the column and the cage. Also, the direct mode of the model with the head column consists of angle bars and stiffeners; the load is distributed directly through these elements. Table 4 shows the case studies and their specifications on which the tests are carried out. Similar values are omitted from the table in order to add more clarity to the depth of the investigation.

As seen from Table 4, there are 15 different case studies, and the effective parameters on the overall strength of the column vary in different cases.

5.1 Results of the FEM analyses

In this section, we examine the numerical analysis modeling output results, including models under axial force.

Two parameters are introduced to study the share of each component in tolerating the axial load. N_c and N_s represent the load born by the column and steel cage. The analyses are presented with the non-dimensional

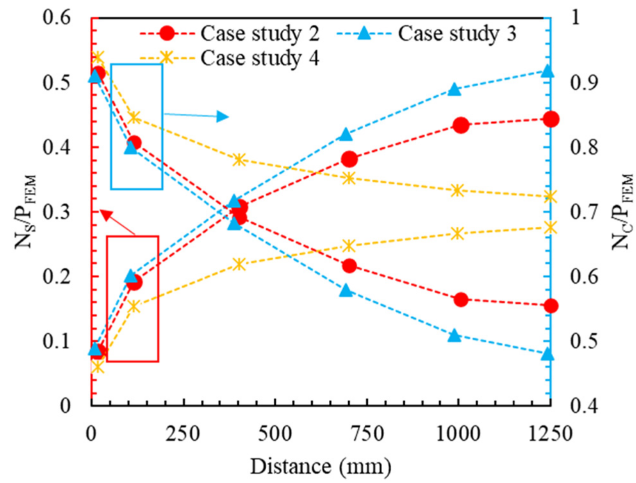

Figure 4: The share of load between the RC column and the cage in case studies 2, 3, and 4.

parameters N_s/P_{FEM} and N_c/P_{FEM}, where P_{FEM} is the overall load on the column.

Figure 4 shows the share of load bearing in case studies 2, 3, and 4. These models would compare the effect of having various numbers of strips. Case studies 2, 3, and 4 have 5, 7, and 3 strips, respectively. Figure 4 shows that the steel cages in case studies 2, 3, and 4 would bear 45, 52, and 28% of the total load at the end of the column. Therefore, the result of increasing the number of strips is an increase in the axial load capacity of the column.

The next parameter to investigate is the size of the strips. The strips' size is a significant parameter in the

Table 4: Selected case studies to study under the axial force

Case study	Angles	Strips (mm^3)	Number of strips	f_c (MPa)	f_y (MPa)
1	—	—	—	8.3	—
2	∟80.8	270 × 160 × 8	5	*	275
3	*	*	7	*	*
4	*	*	3	*	*
5	*	270 × 120 × 8	5	*	*
6	*	270 × 200 × 8	8	*	*
7	∟60.6	270 × 160 × 8	*	*	*
8	∟100.10	*	*	*	*
9	∟80.8	270 × 160 × 6	*	*	*
10	*	270 × 160 × 10	*	*	*
11	*	270 × 160 × 8	*	12	*
12	*	*	*	16	*
13	*	*	*	8.3	355
14	*	*	*	*	235
15	*	*	*	*	275

*The value is equal to the above item.

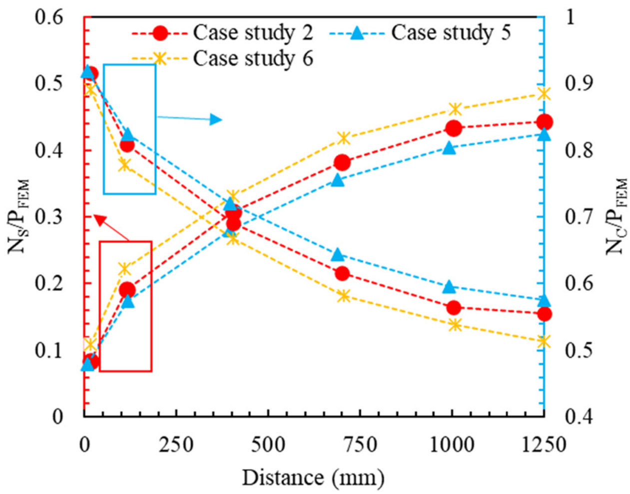

Figure 5: The share of load between the RC column and the cage in case studies 2, 5, and 6.

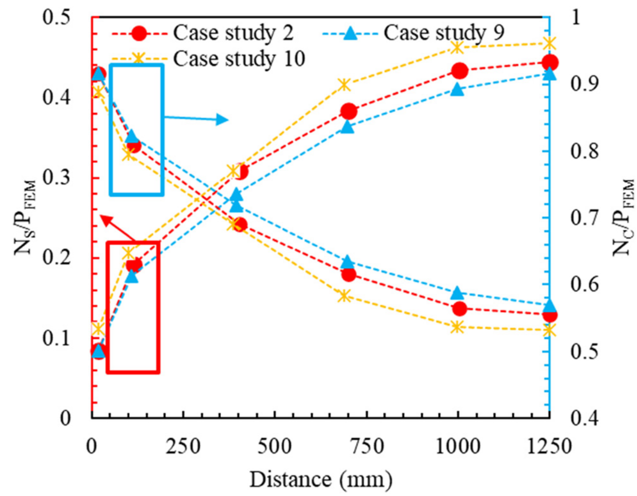

Figure 7: The share of load between the RC column and the cage in case studies 2, 9, and 10.

load-bearing and transmission of the load to the steel cage. Therefore, in Figure 5, the values of the share of load absorbed by the cage with 120, 160, and 200 mm are presented. The results show that the steel cage of the column with a 120 mm strip bears 42%, and that of the column with a 160 mm strip is 45%. Similarly, by increasing the strip size to 200 mm, the steel cage bearing becomes 48%. The results show that increasing the strips' size improves the steel cage capacity. By augmenting the size of the strips, the effect of confinement caused by the strips will improve, and the transmission of load will increase.

Another effective parameter in steel cages is the angle's size. It is observed that by increasing the angles' size, the column resistance increases. Figure 6 shows the effect of the angle size for samples with angle sizes of 60, 80, and 100 mm, and the share of the load absorbed by the steel cage for these values is 39, 45, and 50%, respectively. Also, increasing the angle's size would amplitude the effect of confinement, which is favorable. However, the negative effect is that it decreases the transmission of the load. This is because when the angle's size increases, the weaker parts would be the yield stress of strips.

The thickness of the steel strips has a marginal impact on the behavior of the reinforced column, as can be seen in Figure 7, and the load absorption rate of the steel cage when using strips with a thickness of 8 mm is 45%, which is 43% in the 6 mm strip, and the 10 mm strip has reached 47%.

Figure 8 shows that when the compressive strength of RC is 3.8 MPa, the share of the cage is 45% of the total

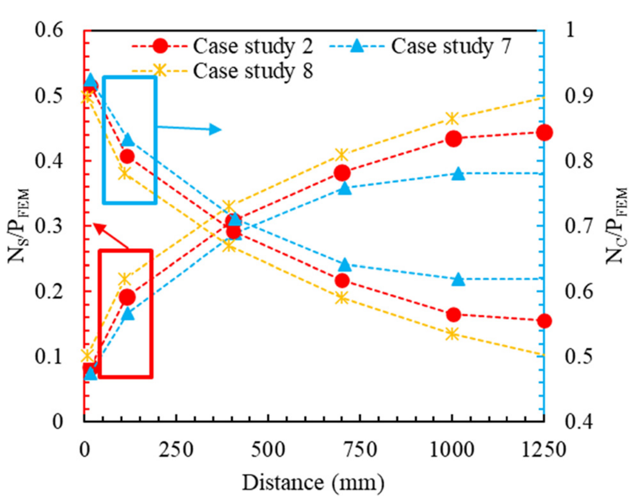

Figure 6: The share of load between the RC column and the cage in case studies 2, 7, and 8.

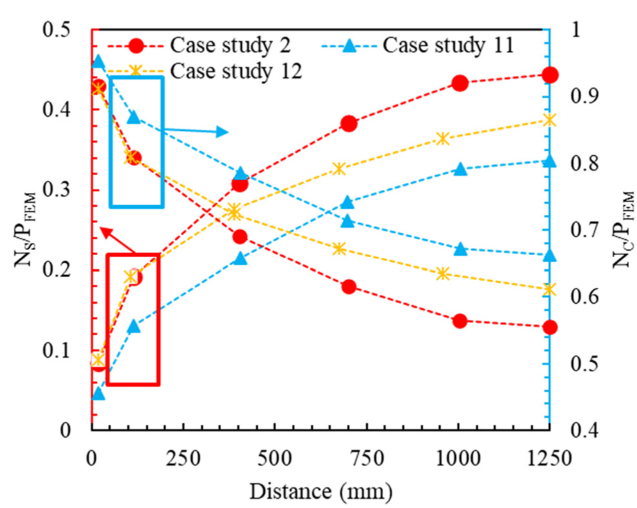

Figure 8: The share of load between the RC column and the cage in case studies 2, 11, and 12.

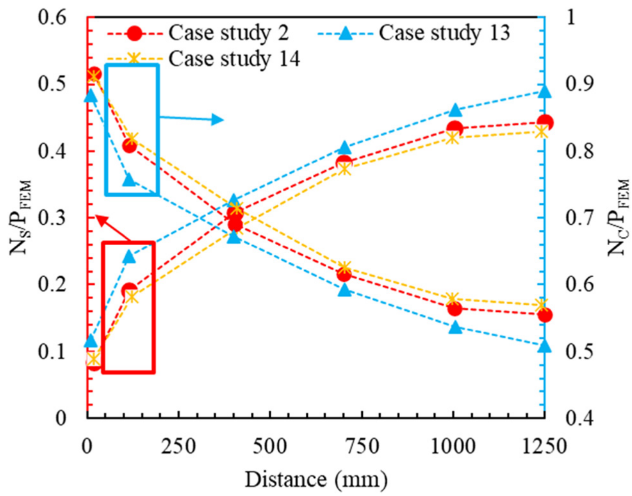

Figure 9: The share of load between the RC column and the cage in case studies 2, 13, and 14.

load of the column, which is reduced to 39 and 34 in samples with compressive strength of 12 and 16 MPa, respectively. It is believed that strengthening the RC is more effective in columns with low compressive strength.

The effect of the material on the steel cage is also investigated. As the material change, the mechanical properties of the structure alter. According to Figure 9, the load absorption rate of the cage when using steel with a yield stress of 275 MPa was 45%, and this value reached 43% at a yield stress of 235 MPa and 48% at a yield stress of 355 MPa, which shows the partial effect of this parameter on the behavior of the reinforced column. The structure designers should highly consider this since the cage with high-yield stress is very expensive.

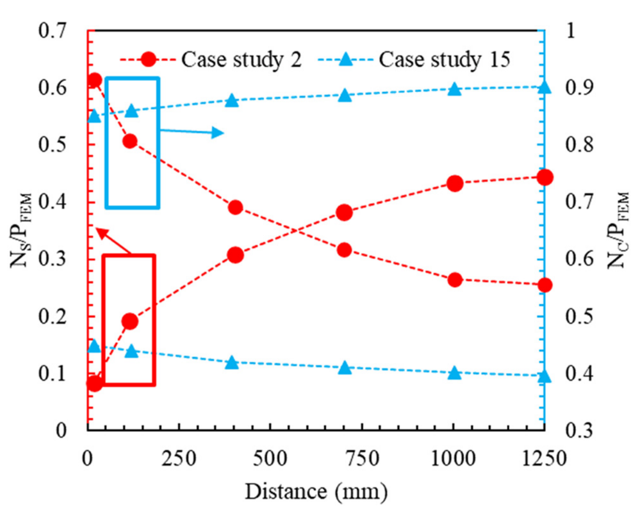

Figure 10: The share of load between the RC column and the cage in case studies 2 and 8.

Table 5: Hyperparameters of N_c/P_{FEM}

ANN parameters	Value
Learning rate	0.01
Hidden layer	128, 128, 64, 32
Activation function of the last layer	ReLU
Batch size	8
Number of epochs	20,000

As was mentioned earlier, the RC head would help stabilize the force exerted on the two ends of the column. Therefore, the RC heads are added to the basic structure of case study 2, and the results are further compared. Using the column head in the joint causes the damage to be transferred from the critical point of the column to other parts. Also, the use of this element causes a significant augmentation in the final load capacity of the RC column. Figure 10 illustrates that the load share of the steel cage in the sample with the column head has increased from 45 to 60% [35].

6 Discussion

The results of the numerical modeling are used to propose predictive models for two parameters, namely, N_c/P_{FEM} and N_s/P_{FEM}. The results of various cases are gathered and split into 70–30% groups. About 70% of the data is

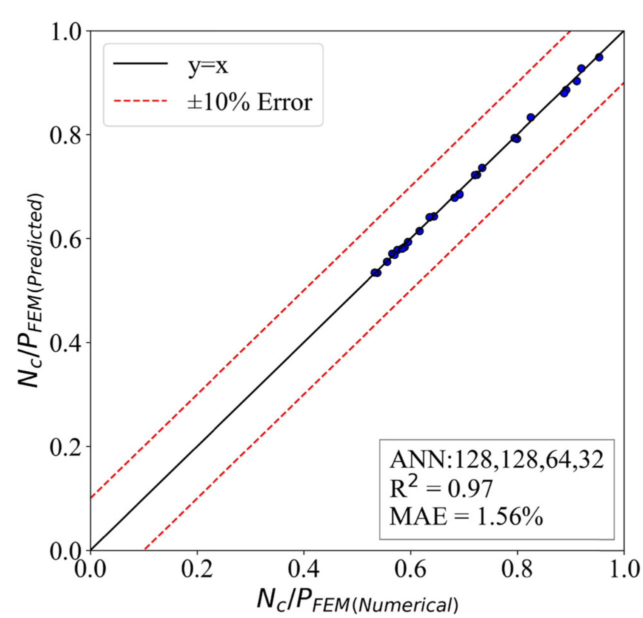

Figure 11: The ANN model for the prediction of N_c/P_{FEM}.

Table 6: Hyperparameters of the N_s/P_{FEM}

ANN parameters	Value
Learning rate	0.01
Hidden layer	32, 64, 128, 64, 32
Activation function of the last layer	Linear
Batch size	16
Number of epochs	30,000

used to train the ANN, and 30% is employed to test the predictive model. It should be mentioned that the model is only trained on the training set, so the testing data points are unseen for the model. In order to optimize the model, we have utilized hyperparameter tuning [36,37].

In the hyperparameter tuning process, the parameters of the ANN model include the number of hidden layers, number of neurons, batch size, number of epochs, and activation function. The accuracy of the model is measured using MAE and R^2. These two parameters are defined as follows [29]:

$$\mathrm{MAE} = \frac{1}{n}\sum_{i=1}^{n}\frac{|Y_i - \hat{Y}_i|}{Y_i} \times 100\%, \quad (1)$$

$$R^2 = 1 - \frac{\sum(Y_i - \hat{Y}_i)^2}{\sum(Y_i - \bar{Y})}, \quad (2)$$

where $\bar{Y}$ is the mean of the data, Y_i is the real value, and $\hat{Y}_i$ is the predicted value.

The final model for N_c/P_{FEM} is presented in Table 5. All the hyperparameters are also included in the table.

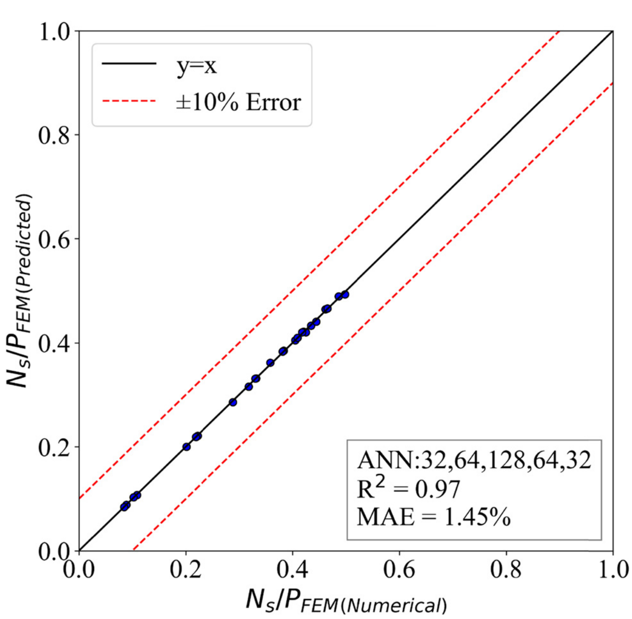

Figure 12: The ANN model for the prediction of N_s/P_{FEM}.

The overall number of data points is 85, where 59 are used for training and 26 are used for testing. Figure 11 indicates the predictions of N_c/P_{FEM}. We have selected mechanical properties of the column, number of strips, size of the strip, and angle size as the input for the predictive model. Based on Figure 11, the hidden layer structure for N_c/P_{FEM} is 128, 128, 64, 32. The metrics of the model are MAE and R^2 whose values are 1.56% and 0.97, respectively. The ANN model is able to predict the numerical modeling data accurately.

Also, the hyperparameters for N_s/P_{FEM} are shown in Table 6.

The model for N_s/P_{FEM} uses 32, 64, 128, 64, 32 structure for its hidden layers, according to Figure 12. The MAE of the model is 1.45%, and the R^2 of the model is 0.97. The results of both models prove to be satisfactory since they are very close to the numerical results. Therefore, it is logical to assume that predictive models could replace the time-consuming numerical modeling and experimental testing in the near future, although more research should be devoted to it.

7 Conclusion

In this article, ABAQUS is employed to study an RC column using the FEM. A steel cage is used for increasing the load bearing of the structure. In order to better understand the physics of adding the steel cage, the impact of the number of strips, the thickness of strips, angles, using RC heads, the size of strips, the mechanical properties of RC, and the cage's mechanical parameters are investigated. Moreover, ANNs are used to propose predictive models for N_c/P_{FEM} and N_s/P_{FEM} and the results of the modeling are used. The model is optimized to achieve the best result, *i.e.*, hyperparameter tuning. The highlight of the results is presented in the following:

- The number of steel strips has a noticeable effect on the final axial load of the column. This parameter plays a significant role in both the confinement of the column and the transmission of the load between the column and the cage. By increasing the size of the strips, one can reduce the effect of slipping.
- By increasing the angle size, the hardness of the steel increases, and it absorbs more load. Increasing this parameter also puts the structure's failure under the strips' yield stress.
- The thickness of the steel strips has a small effect on changing the axial load capacity of the reinforced column.

- Increasing or decreasing the yield stress has a small contribution to changing the steel cage's carrying capacity and the column's final load. This parameter should be considered, especially in the designing phase of the structure, due to the high expenses of the steel cages.
- The two ends of the columns are the weakest part of the structure, so adding the RC heads was investigated to check whether they could help mitigate this effect. Adding the head of the column to the end of the sample causes a direct load transfer mechanism so that this element causes a direct angular load on the top of the column and increases the load transfer.
- In order to add more insight into the load bearing of the retrofitted RC columns, the data from the present study are used to propose predictive models for N_c/P_{FEM} and N_s/P_{FEM} using ANNs. All the hyperparameters, such as the number of hidden layers, activation function, batch size, epochs, *etc.*, are tuned to achieve the best results. The predictive models proved to be a very accurate and reasonable method to propose because the models had a high accuracy of MAE of less than 2% and R^2 of higher than 0.96.

Acknowledgements: The author would like to thank the Middle Technical University, Technical Institute of Baquba, Diyala, Iraq, for supporting the present work.

Funding information: The author did not receive any funding.

Author contributions: Larah R. Abdulwahed: conceptualization, writing, revision, and editing.

Conflict of interest: The author declares that there is no conflict of interests.

Ethical approval: This article does not contain any studies with human participants or animals performed by the author.

References

[1] Desprez C, Mazars J, Kotronis P, Paultre P, Roy N, Boucher-Trudeau M. Retrofitting reinforced concrete structures with FRP: Numerical simulations using multifiber beam elements. In: Papadrakakis M, Lagaros ND, Fragiadakis M, editors. ECCOMAS Thematic Conference on Computational Methods in Structural Dynamics and Earthquake Engineering (COMPDYN 2009); 2009 June 22-24; Rhodes, Greece. HAL, 2009.
[2] Jia J, Zhao L, Wu S, Wang X, Bai Y, Wei Y. Experimental investigation on the seismic performance of low-level corroded and retrofitted reinforced concrete bridge columns with CFRP fabric. Eng Struct. 2020;209:110225.
[3] Somarathna HMCC, Raman SN, Mohotti D, Mutalib AA, Badri KH. Behaviour of concrete specimens retrofitted with bio-based polyurethane coatings under dynamic loads. Constr Build Mater. 2021;270:121860.
[4] Alexander M, Beushausen HD, Dehn F, Moyo P, editors. Concrete repair, rehabilitation and retrofitting. London, UK: Taylor & Francis; 2006.
[5] Facconi L, Lucchini SS, Minelli F, Plizzari GA. Analytical model for the in-plane resistance of masonry walls retrofitted with steel fiber reinforced mortar coating. Eng Struct. 2023;275:115232.
[6] Sharba AAK, Hussain HD, Abdulhussain M. Retrofitting of RC beams using FRP techniques: a review. IOP Conf Ser: Mater Sci Eng. 2021;1090:012054.
[7] Saghafi MH, Golafshar A. Seismic retrofit of deficient 3D RC beam–column joints using FRP and steel PT rods. Mater Struct. 2022;55(8):1–16.
[8] Meghdadian M, Ghalehnovi M. Retrofitting of core reinforced concrete shear wall system with opening using steel plates and FRP sheets, A case study. Int J Steel Struct. 2022;22(4):920–39.
[9] Thai DK, Pham TH, Nguyen DL. Damage assessment of reinforced concrete columns retrofitted by steel jacket under blast loading. Struct Des Tall Spec Build. 2020;29(1):e1676.
[10] Hanifehzadeh M, Aryan H, Gencturk B, Akyniyazov D. Structural response of steel jacket-UHPC retrofitted reinforced concrete columns under blast loading. Materials. 2021;14(6):1521.
[11] Thermou GE, Papanikolaou VK, Hajirasouliha I. Structural performance of RC columns retrofitted with steel-reinforced grout jackets under combined axial and lateral loading. Eng Struct. 2021;245:112946.
[12] Zhang D, Li N, Li ZX, Xie L. Rapid repair of RC bridge columns with prestressed stainless-steel hoops and stainless-steel jackets. J Constr Steel Res. 2021;177:106441.
[13] Deng BY, Liu X, Yu KQ, Li LZ, Chen Y. Seismic retrofitting of RC joints using steel cage and haunch with bolted steel plate. Structures. 2022;43:285–98.
[14] Frangou M, Pilakoutas K, Dritsos S. Structural repair/strengthening of RC columns. Constr Build Mater. 1995;9(5):259–66.
[15] Aboutaha RS, Engelhardt MD, Jirsa JO, Kreger ME. Retrofit of concrete columns with inadequate lap splices by the use of rectangular steel jackets. Earthq Spectra. 1996;12(4):693–714.
[16] Cirtek L. RC columns strengthened with bandage—experimental programme and design recommendations. Constr Build Mater. 2001;15(8):341–9.
[17] Xiao Y, Wu H. Retrofit of reinforced concrete columns using partially stiffened steel jackets. J Struct Eng. 2003;129(6):725–32.
[18] Wu YF, Liu T, Oehlers DJ. Fundamental principles that govern retrofitting of reinforced concrete columns by steel and FRP jacketing. Adv Struct Eng. 2006;9(4):507–33.

[19] Adam JM, Giménez E, Calderón PA, Pallarés FJ, Ivorra S. Experimental study of beam-column joints in axially loaded RC columns strengthened by steel angles and strips. Steel Compos Struct. 2008;8(4):329–42.
[20] Montuori R, Piluso V. Reinforced concrete columns strengthened with angles and battens subjected to eccentric load. Eng Struct. 2009;31(2):539–50.
[21] Adam JM, Ivorra S, Pallarés FJ, Giménez E, Calderón PA. Axially loaded RC columns strengthened by steel caging. Finite element modelling. Constr Build Mater. 2009;23(6):2265–76.
[22] Calderón PA, Adam JM, Ivorra S, Pallarés FJ, Giménez E. Design strength of axially loaded RC columns strengthened by steel caging. Mater Des. 2009;30(10):4069–80.
[23] Tarabia AM, Albakry HF. Strengthening of RC columns by steel angles and strips. Alex Eng J. 2014;53(3):615–26.
[24] Belal MF, Mohamed HM, Morad SA. Behavior of reinforced concrete columns strengthened by steel jacket. HBRC J. 2015;11(2):201–12.
[25] Ong CB, Chin CL, Ma CK, Tan JY, Awang AZ, Omar W. Seismic retrofit of reinforced concrete beam-column joints using various confinement techniques: A review. Structures. 2022;42:221–43.
[26] Maheswaran J, Chellapandian M, Arunachelam N. Retrofitting of severely damaged reinforced concrete members using fiber reinforced polymers: A comprehensive review. Structures. 2022;38:1257–76.
[27] Dai KY, Yu XH, Qian K, Wang DY. Deformation capacity of FRP retrofitted reinforced concrete columns with corroded reinforcing bars. Eng Struct. 2022;254:113834.
[28] Xie L, Wang X, Zeng D, Jia J, Liu Q. Resilience-based retrofitting of adjacent reinforced concrete frame–shear wall buildings integrated into a common isolation system. J Perform Constr Facilities. 2022;36(1):04021100.
[29] Shin J, Park S. Optimum retrofit strategy of FRP column jacketing system for non-ductile RC building frames using artificial neural network and genetic algorithm hybrid approach. J Build Eng. 2022;57:104919.
[30] Dabiri H, Rahimzadeh K, Kheyroddin A. A comparison of machine learning-and regression-based models for predicting ductility ratio of RC beam-column joints. Structures. 2022;37:69–81.
[31] Almustafa MK, Nehdi ML. Machine learning model for predicting structural response of RC columns subjected to blast loading. Int J Impact Eng. 2022;162:104145.
[32] Falcone R, Ciaramella A, Carrabs F, Strisciuglio N, Martinelli E. Artificial neural network for technical feasibility prediction of seismic retrofitting in existing RC structures. Structures. 2022;41:1220–34.
[33] Mander JB, Priestley MJ, Park R. Theoretical stress-strain model for confined concrete. J Struct Eng. 1988;114(8):1804–26.
[34] Adam JM, Ivorra S, Gimenez E, Moragues JJ, Miguel P, Miragall C, et al. Behavior of axially loaded RC columns strengthened by steel angles and strips. Steel Compos Struct. 2007;7(5):405–19.
[35] Garzon-Roca J, Adam JM, Calderon PA. Behaviour of RC columns strengthened by steel caging under combined bending and axial loads. Constr Build Mater. 2011;25(5):2402–12.
[36] Eskandari E, Alimoradi H, Pourbagian M, Shams M. Numerical investigation and deep learning-based prediction of heat transfer characteristics and bubble dynamics of subcooled flow boiling in a vertical tube. Korean J Chem Eng. 2022;39(12):3227–45.
[37] Alimoradi H, Eskandari E, Pourbagian M, Shams M. A parametric study of subcooled flow boiling of Al2O3/water nanofluid using numerical simulation and artificial neural networks. Nanoscale Microscale Thermophys Eng. 2022;26(2–3):129–59.